The Role of Covalent Functionalization in the Thermal Stability and Decomposition of Hybrid Layered Hydroxides

Víctor Oestreicher, Gonzalo Abellán and Eugenio Coronado

Abstract

The room temperature synthesis of two Co-based hybrid layered hydroxides containing the same organic ligand (suberate [Sub]), one connected through purely electrostatic interactions (CoAl layered double hydroxide [LDH]), and the other covalently functionalized (α-Co^{II} simonkolleite phase) has been carried out. The magnetic properties exhibit an acute difference in the magnetization temperatures (from ≈10 K for the CoAl-LDH to ≈55 K for the α-Co^{II}). Moreover, the role of the covalent functionalization in the thermal stability and the decomposition has been investigated by a forefront characterization tool consisting of thermogravimetric analysis coupled with gas chromatography and mass spectrometry (TG–GC–MS). The LDH exhibits a higher thermal stability of ≈50 ºC with broad mass loss steps, whereas the water molecules interact stronger with the α-Co^{II}(Sub) hybrid, suggesting a higher confinement in the interlayer space. Interestingly, at higher temperatures (>400 ºC), the α-Co^{II}(Sub) gives rise to the selective formation of cycloheptanone, in contrast to the LDH phase leading to different carbonyl containing compounds. These findings offer new fundamental insights into the thermal behavior of hybrid materials based on layered hydroxides, highlighting the important role of covalent functionalization in its properties.

Hybrid organic–inorganic materials represent one of the hottest research topics in materials science. The close structure–property relationship exhibited in these materials gives rise to a wide variety of applications in fields ranging from biomedicine, catalysis or magnetism to energy storage and conversion.[1-4]

Layered and 2D systems, especially those based on earth-abundant metals, are playing a key role in the hybrid materials family. The possibility of combining their physical, chemical, and mechanical properties, and the precise control over their structures, placed them in a privileged position.[5-12] Among others, layered hydroxides (LHs) offer a broad range of possibilities due to their tunable chemistry, which allows to modify at will both the inorganic layers and (in)organic intercalated anions.[13] Layered double hydroxides (LDHs) constitute the most famous member of the LHs family exhibiting purely electrostatic sheet/anion interactions. These lamellar systems display *hydrotalcite*-like structures composed of positive charged sheets where both M^{II} and M^{III} octahedral cations can be tuned.[14] In line with that, hybrid LDHs have been proposed, among others, used for stimuli-responsive materials, or as a precursor for the synthesis of carbon-based nanocomposites of interest in energy storage and conversion.[15-17] In all cases,

the main properties are governed by the chemical nature of both components (inorganic host and organic guest) and the interaction between them, which is always electrostatic. In the search of new levels of functionality and complexity, different functionalization strategies have been explored, mainly based in the covalent functionalization (e.g., sylilation) of the interface, resulting in improved absorption properties but slight modifications of the magnetic or electrochemical properties.[18]

Along this front, α-Co^{II} hydroxides (or *simonkolleite*-like structures) are positioned as key members in the LHs family, because they can be considered as naturally occurring covalently functionalized LHs. They present two coordination environments, octahedral centers –Co^{II}(O_h)– within the layers, as in the case of LDHs and tetrahedral ones –Co^{II}(T_d)– attached to both sides by 3OH bridges. The fourth position can be used to graft different inorganic to organic ligands (**Scheme 1**).[19] The electronic and magnetic properties can be tuned by changing ligand and/or Co^{II}(T_d) ratio, resulting in more conductive systems (mainly by ligand to metal charge transfer) with higher magnetization temperatures (T_M) as to the related LDHs.[20-22] Moreover, as recently reported by our group, in hybrid α-Co^{II} hydroxydicarboxylates, $Co_5(OH)_8[(CH_2)_n(COO)_2]$ with *n* ranging from 1 to 8, the magnetic behavior can be dramatically modified by changing the parity of the organic linker: whereas odd members present T_M < 20 K the even ones have T_M > 55 K.[23]

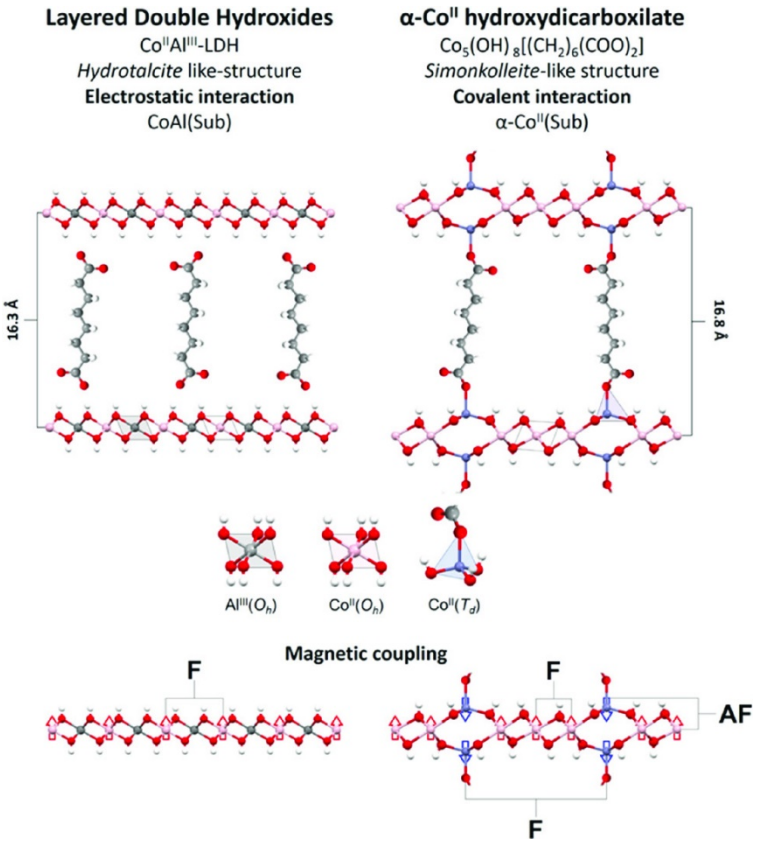

Scheme 1

Schematic representation of the crystalline structures of the LHs herein studied. LDHs composed by Co^{II} and Al^{III} located both in octahedral environments, exhibiting purely electrostatic interactions between the positively charged layers and anions (left panel). α-Co^{II} hydroxydicarboxylates consisting of both octahedral (O_h) and

tetrahedral (T_d) Co^{II} atoms present covalent bonding between the $Co^{II}(T_d)$ centers and carboxylic groups (right panel). As a matter of comparison, both LHs contain suberate, $[(CH_2)_6(COO)_2]^{2-}$ (Sub), as interlayer anion. Intralayer magnetic coupling in the studied LHs: AF and F coupling.

These results demonstrate that the nature of the interaction between the inorganic layers and the organic guest is crucial for determining the properties of these LHs. However, little is known about the influence of the covalent bonds in thermal stability and decomposition behavior of these hybrid materials.

In this article, we have studied in detail the influence of the electrostatic and covalent interactions in the structure, magnetism, and thermal behavior of a CoAl-LDH and an α-Co^{II} hydroxide intercalated with suberic acid ($(CH_2)_6(COOH)_2$ (Sub)). The experimental results show marked differences in magnetism, a higher thermal stability of ≈50 °C for the CoAl(Sub) LDH, as well as a differentiated thermal decomposition behavior, in which the presence of covalent bonds originates the selective formation of cycloheptanone at ≈400 °C, derived from the suberic acid. This work provides fundamental information about the decomposition behavior of cobalt-based LHs, highlighting how the nature of the interactions between the inorganic/organic constituents may alter the physicochemical properties. This knowledge will pave the way for the precise tuning of the properties of hybrid LHs,[24] and will offer new possibilities in the molecular design of precursors for the preparation of carbon-based nanocomposites.[17, 25]

To study the role of the covalent functionalization in hybrid cobalt (II) LHs, two different systems have been studied. On the one hand, a purely electrostatic system such as a CoAl-LDH containing a dicarboxylic anion (Scheme **1**) and on the other hand, a *simonkolleite*-like phase where the dicarboxylic anion is bridging consecutive inorganic layers through covalent bonding: α-Co^{II} hydroxydicarboxylates. In this way, the comparison between electrostatic and covalent interactions was studied for CoAl-LDH and α-Co^{II} hydroxides containing the same dicarboxylic molecule, i.e., suberate: $[(CH_2)_6(COO)_2]^{2-}$.

The samples were synthesized at room temperature by the so-called *Epoxide Route*, recently developed by some of us.[26] This method has been successfully used for the synthesis of several LHs,[21, 27] LDHs[28] and their hybrid forms,[29] or metal organic frameworks (MOFs).[30] In this report, both solid samples were obtained in a one-pot procedure under environmental conditions by aging aqueous solutions for 48 h at room temperature (see Experimental Section, Supporting Information).

As a first step, the solid phases were characterized by powder X-ray diffraction (PXRD). **Figure 1A** confirms the layered structures by the presence of the typical (*00 l*) reflections at lower *2-theta* values, associated with basal space distances (d_{BS}). In both samples, a d_{BS} of around 16–17 Å was obtained. In the case of α-Co^{II}(Sub), the slightly higher d_{BS} can be related to the presence of $Co^{II}(T_d)$ attached to the hydroxylated layers.[28] At higher 2-*theta* values, the (*110*) reflections were observed, which are associated with the intralayer distance (*a* parameter). A clear shift towards higher 2-*theta* values was observed for the CoAl-LDH sample (Figure **1A**, *inset*), in concordance by the replacement of Co(II) by Al(III) within the layers

($RCo(II)Oh$=0.745 ÅRCo(II)Oh=0.745 Å; $RAl(III)Oh$=0.535 ÅRAl(III)Oh=0.535 Å).[31] **Table 1** shows the structural parameters obtained from PXRD.

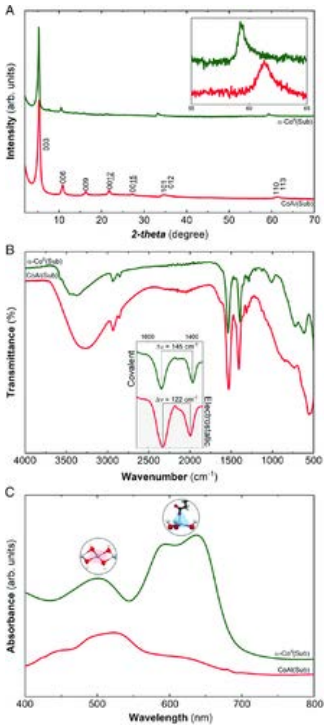

Figure 1

A) PXRD patterns, B) ATR–FTIR, and C) UV–vis diffuse reflectance spectra for CoAl-LDH (red) and α-Co^{II} hydroxydicarboxylate (green) containing suberate as interlayer anion, CoAl(Sub) and α-Co^{II}(Sub), respectively.

Table 1. Structural parameters for the obtained samples. Basal space distances calculated as d_{BS} = 1/3·(d_{003} + 2·d_{006} + 3·d_{009}), *c* parameter estimated as *c* = 3·d_{BS}, and *a* parameter obtained as a = 2·d_{110}

Sample	***d*** **$_{BS}$ [Å]**	***c*** **[Å]**	***a*** **[Å]**
CoAl(Sub)	16.4	49.2	3.02
α-Co^{II}(Sub)	16.8	50.4	3.12

Attenuated total reflectance Fourier-transform infrared spectroscopy (ATR–FTIR) was used to confirm the incorporation of the organic molecules into the hybrids (Figure **1B**). The two signals observed at ≈2935 and 2855 cm^{-1} are attributed to asymmetric and symmetric CH_2 stretching vibrations. The strong bands at ≈1750–1250 cm^{-1} are assigned to asymmetric and symmetric stretching modes of the carboxylic groups.[32] The difference between both bands, Δ*v* = v_{asym} − v_{sym}, can be useful for revealing the carboxylate

interaction. Indeed, the lower Δν for CoAl(Sub) sample (122 cm^{-1}) suggests ionic interaction; in turn an unidentate coordination can be proposed for α-Co^{II}(Sub) (Scheme **1** and Figure **1B**–*inset*) in view of the higher Δν (145 cm^{-1}).[33, 34] Finally, the broad band centered at ≈3450 cm^{-1} is attributed to the presence of interlayer water molecules (O⋯H stretching modes),[32] whereas the bands below 1000 cm^{-1} are related to M⋯O stretching and M⋯OH bending vibrations.[35]

UV–vis diffuse reflectance spectroscopy is a suitable technique in LHs characterization as it can provide information about both metallic coordination environments[36] and the type of functionalization.[21, 23] In the case of the CoAl(Sub) sample, only a broad peak around 525 nm was observed denoting the exclusive presence of Co^{II}(O_h). In the case of α-Co^{II}(Sub) sample, beside this peak, the appearance of a strong band with twin-peaks at 595 and 637 nm confirm the presence of Co^{II}(T_d) (Figure **1C**).[19, 21] The position of this band is sensible to the coordinated anion as it was reported for α-Co^{II} hydroxyhalide compounds.[21] Therefore, these techniques allow to confirm the absence of chloride, in agreement with energy dispersive X-ray spectroscopy (EDS) measurements (no traces of Cl were observable, data not shown).

All techniques confirm the obtaining of pure hybrid LHs in both structures *hydrotalcite*-like CoAl-LDHs (with electrostatic interaction with the organic molecule) and *simonkolleite*-like α-Co^{II} hydroxydicarboxylate (with covalent interaction with the organic molecule).

The magnetism in LHs depends mainly on two factors. On the one hand, intralayer magnetic coupling between the cations mediated by superexchange interactions through hydroxo bridges and on the other hand, the less intense interlayer dipolar interactions. Concerning the former, in the case of the CoAl-LDH, only intralayer ferromagnetic (F) coupling between Co was expected.[37] However, in the case of the α-Co^{II} hydroxides, a more complex behavior may take place due to the coexistence of different magnetic sublattices arising from the different Co environments.[21, 22] Specifically, F interactions between Co in identical coordination environments ($O_h - O_h$ and $T_d - T_d$) and antiferromagnetic (AF) interactions between Co in different environments ($O_h - T_d$) are expected, leading to uncompensated moments, which results in ferrimagnetic layers (Scheme **1**).[21, 22]

The magnetic results are shown in **Figure 2** and **Table 2**. In the case of CoAl-LDH, fitting of the inverse of the magnetic susceptibility ($1/\chi$) according to a Curie–Weiss law in the 50–300 K region results in a negative value of the Weiss constant (ϑ_{CW} = −9.3 K), which does not seem to be due to the predominance of AF interactions but due to the orbital contribution coming from octahedral Co(II). Magnetization temperature (T_M, defined as the point where $\chi''_M \neq 0$) of 5.7 K and coercive fields (H_c) lower than 0.1 kOe were obtained, as expected according to previous reports on CoAl-LDH intercalated with *n*-alkyl sulphate molecules.[37] However, the magnetism in the case of α-Co^{II} hydroxydicarboxylate depicts an striking different behavior: in α-Co^{II}(Sub) sample, the fitting of the Curie–Weiss law in the 200–300 K region yields a ϑ_{CW} value of 66.4 K, with T_M = 60 K and H_c bigger than 10 kOe (see Figure **2** and Table **2**). Therefore, it is

important to highlight that covalent functionalization drives the coexistence of two magnetic sublattices (also known as triple-deck structures),[5, 21, 22] O_h and T_d, proper in α-Co^{II} hydroxides, offering a new coupling that pushes the magnetic transition to higher temperatures. In both hybrids, the absence of extrinsic magnetic impurities, such as Co^{III} spinels, was confirmed by the temperature-independent component in $\chi_M \cdot T$ assuring the purity of the LHs.[38, 39]

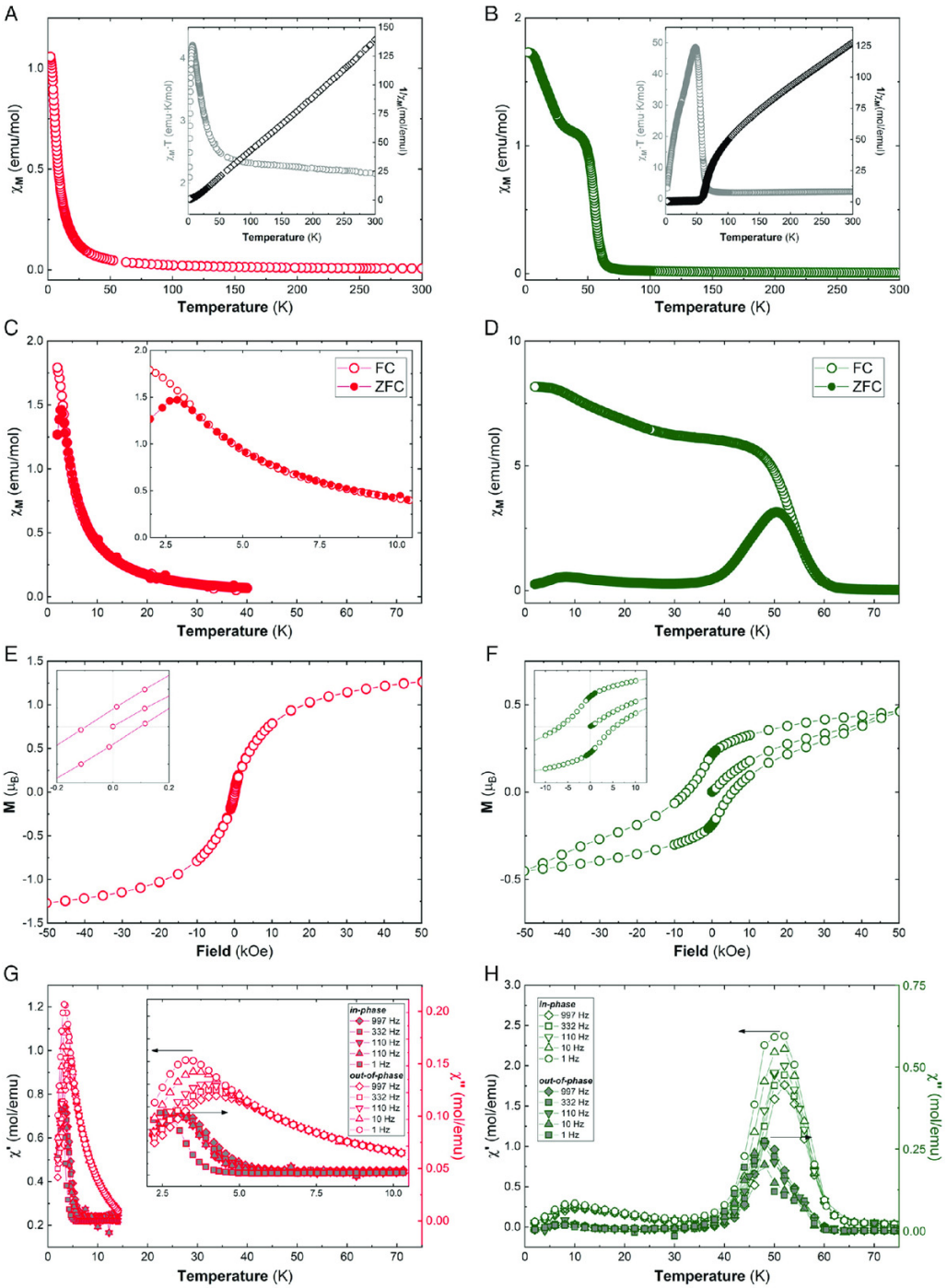

Figure 2

Magnetic characterization for CoAl-LDH (left panel, red) and α-Co^{II} hydroxydicarboxylate (right panel, green) hybrids containing suberate as interlayer anion. A,B) Magnetic susceptibility as a function of temperature (χ_M vs T) with an external applied field of 1000 Oe; the inset shows the thermal dependence of $\chi_M \cdot T$ and the fitting of the $1/\chi_M$ to a

Curie–Weiss law. C,D) Field-cooled and zero-field-cooled (FC/ZFC) with an external applied field of 100 Oe. E,F) Hysteresis cycle at 2 K; the inset shows the low field region. G) Thermal dependence of dynamic susceptibility for the in-phase (χ_M') and the out-of-phase (χ_M'') signals at 1, 10, 110, 332, and 997 Hz (F).

Table 2. Main magnetic data and parameters for CoAl-LDHs and α-Co^{II} hydroxycarboxylate containing suberate as interlayer anion. $\chi \cdot T_{RT}$ value at room temperature; experimental Curie constant (C); Weiss constant (ϑ); temperature of the divergence of the ZFC and FC magnetic susceptibility (T_B); temperature for the onset of spontaneous magnetization extracted from the χ''_M plot (T_M); saturation magnetization (M_S); remanence magnetization (M_R); coercive field (H_C)

Samples	$\chi \cdot T_{RT}$ [emu K mol^{-1}]	C [emu K mol^{-1}]	ϑ [K]	T_B [K]	T_M [K]	M_S [μ_B]	M_R [μ_B]	H_C [Oe]
CoAl(Sub)	2.15	2.1	−9.3	2.9	5.7	1.27	0.23	95
α-Co^{II}(Sub)	2.33	2.9	66.4	52	60	0.46	0.21	12075

Once observed the influence of the different structures on the magnetic properties, we have conducted a thermogravimetric study to determine the role of the electrostatic/covalent interactions in the thermal stability of the hybrids. The thermal decomposition was followed under oxidizing conditions at 5 °C min^{-1} (Figure S1, Supporting Information); both samples show two main weight loss steps. Although the first step below 100 °C is attributed to the loss of both physisorbed and interlayer water,[13] the second one, centered at around 250 °C, is ascribed to the oxidation of the organic molecules and the dehydroxylation of structural OH groups, which results in the collapse and decomposition of the hybrid layered structure.[19] As can be observed, although the decomposition of the covalent functionalized hybrid takes place at 228 °C, the decomposition temperature for the hybrid CoAl-LDH occurs at significantly higher temperatures, 264 °C. These results demonstrate the higher stability under oxidative conditions of the hybrid LDHs based on electrostatic anchoring (Figure S1, Supporting Information). In fact, this can be related with the presence of Co^{II}(T_d) which would be prone to the oxidation.

To gain further information, thermogravimetric analysis coupled with gas chromatography and mass spectrometry (TG–GC–MS) under an inert atmosphere of helium has been used. This is a powerful technique to unveil the thermal stability of the hybrids, as well as the thermal decomposition products and pathways.[21, 25, 40-43]

Figure 3 shows the thermograms, where at least three steps are noticeable in both samples under nonoxidizing conditions. To shed light on decomposition process itself, the evolved gaseous fragments

(20 mL min^{-1}, He as carrier gas) were injected at each decomposition step in a gas chromatography column, where they were separated generating the corresponding elugrams. Subsequently, the respective sample fractions were analyzed by mass spectrometry.

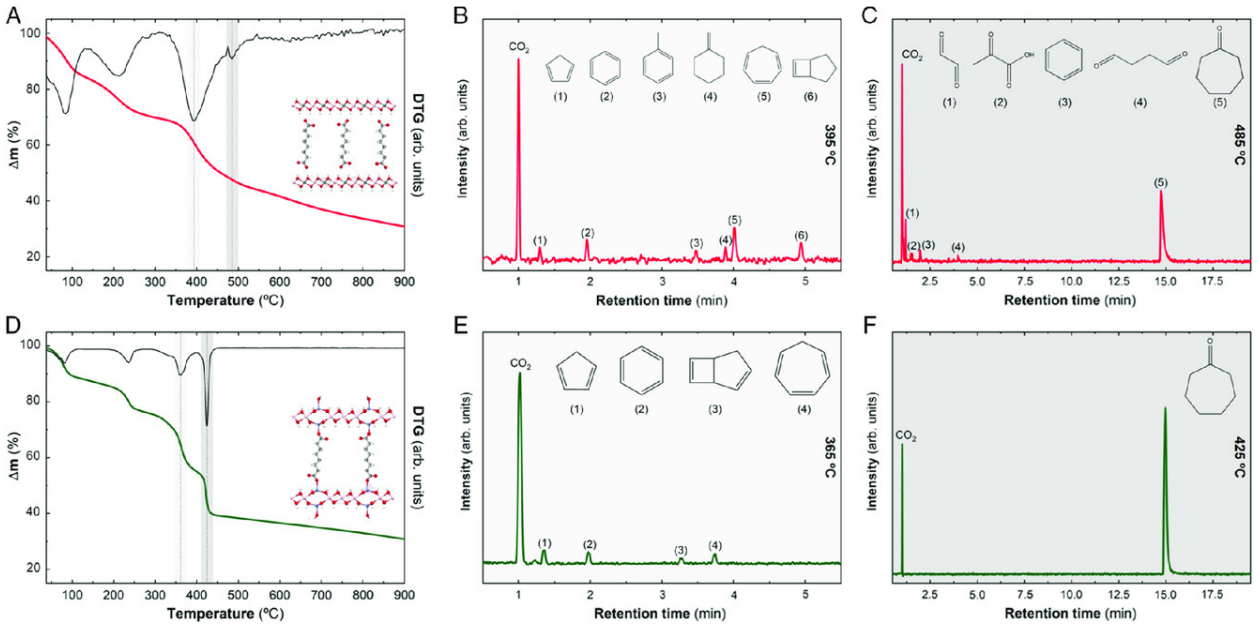

Figure 3

TG–GC–MS characterization. A) TG patterns for CoAl(Sub) (red) and D) α-Co^{II}(Sub) (green) hybrids were recorded at 10 °C/min under inert atmosphere of helium. B,C,E,F) During the decomposition process, the evolved gaseous fragments were injected in a preheated GC column at 40 °C. After chromatographic separation, the molecules were identified by MS.

The first two steps are unambiguously assigned to the physisorbed and intralayer molecules of water. Although the first step is observable at ≈80–85 °C for both samples, the second one takes place at 215 and 235 °C for CoAl(Sub) and α-Co^{II}(Sub), respectively. These results suggest that the physisorbed water molecules behave almost identically; however, a higher interaction of the intralayer water molecules in the case of the *simonkolleite*-like structure is noticeable. Indeed, the first derivative of the TG signal (DTG) is much sharper for α-Co^{II}(Sub), suggesting a more defined environment for the molecules and, therefore, implying a more acute confinement. Related to this phenomenon, it has been recently reported that α-Co^{II} hydroxyhalides exhibit a greater interaction of water molecules within the space between layers as the radius of the anions decreases, resulting in a difference of almost 20 °C in the dehydration temperature.[21]

Up to 300 °C, the decomposition of both hybrids takes place. For CoAl(Sub), the process spans over a wide range of temperatures, 340–530 °C, with a broad maximum and a shoulder in the DTG at 395 and 485 °C, respectively. In turn, for α-Co^{II}(Sub), the decomposition occurs in a narrow range of temperature, 340–445 °C, exhibiting two sharp and well-defined steps at 360 and 425 °C.

Figure 3 shows the elugrams for the injections at 395 and 485 °C for CoAl(Sub) and 365 and 425 °C for α-Co^{II}(Sub), respectively. Figure 3B shows the elugram of CoAl(Sub) obtained from the injection at 395 °C. After a first intense peak related with the releasing of carbon dioxide (CO_2), proper to the decomposition of the organic molecule, different cyclic molecules, namely, cyclopentene, benzene, toluene, methylenecyclohexane, cycloheptatriene, and bicyclo(3.2.0)hept-6-ene are observable. The presence of benzene and toluene can be attributed to the catalytic formation of graphitic carbon, typically observable in the preparation of LDH-based hybrid nanocomposites.[25, 44] Figure 3C shows the elugram of the next injection performed at 485 °C. In this case, after the releasing of CO_2, a new set of four molecules containing carbonyl groups (glyoxal, 2-oxopropionic acid, butandial (succinaldehyde), and cycloheptanone) can be detected, in addition to benzene. Interestingly, the major component of this fraction is a seven-carbon atoms ring: the cycloheptanone.

A similar analysis over the covalently functionalized α-Co^{II}(Sub) was performed by injecting at 365 and 425 °C, respectively. Once again, in the first step of decomposition at 365 °C, the presence of CO_2 is observable (Figure 3E). Then, four different cyclic and unsaturated molecules containing 5, 6, and 7 C atoms are noticeable, as in the case of CoAl(Sub). Remarkably, after injection at 425 °C, only an intense signal of cycloheptanone is observable, in stark contrast to CoAl(Sub) (Figure 3F).

Therefore, we observed that the thermal decomposition products in both hybrids exhibit clear differences, being the most significant one the selective formation of cycloheptanone in the case of the hybrid with covalent interactions. This reaction can be thought as the decarboxylation of suberate moieties and subsequent cyclization to increase the stability of the releasing molecule. Overall, it can be proposed that the catalytic role of Co atoms on the decomposition of Co-based hybrid LHs remains unaltered,[45] but the presence of covalent grafting induces a decrease of the thermal stability of ≈50 °C and results in a more selective decomposition pathway at high (>400 °C) temperatures, leading to the exclusive formation of cyclic ketone derivative of the suberate ligands: cycloheptanone.

In conclusion, two Co-based hybrid LHs containing the same organic ligand (suberate), one connected through purely electrostatic interactions –CoAl(Sub)– and the other covalently functionalized –α-Co^{II}(Sub)–, were synthesized by the *Epoxide Route* in a one-pot reaction at room temperature. The covalent bonding between the *simonkolleite* layers and the COO groups was proved by PXRD, ATR–FTIR, and UV–vis. The influence of the covalent functionalization over the electronic properties of the hybrid is remarkable. Thus, the presence of a tetrahedral environment for Co, characteristic of this phase, strongly influences the magnetic behavior and the increase in the magnetization temperatures from less than 10 K for CoAl-LDH to more than 55 K in the case of α-Co^{II} hydroxydicarboxylates.

Finally, the covalent functionalization has also shown to play a key role in the thermal stability and decomposition of these hybrids. This was studied by TG–GC–MS for the very first time. The result shows that the water molecules interact stronger with the α-Co^{II}(Sub) hybrid denoting a higher confinement for

the molecules in the interlayer space. Regarding the decomposition, a slightly higher thermal stability (<50 °C under oxidizing conditions) was observable for CoAl-LDH hybrid, with more acute mass loss steps for the covalent derivative. In both cases, the catalytic role of Co atoms in the decomposition process under inert conditions results in the formation of graphitic carbon, generating typical aromatic molecules like benzene or toluene. In contrast, at higher temperatures (>400 °C), the α-Co^{II}(Sub) gives rise to the selective formation of cycloheptanone. These results highlight the important role of covalent functionalization on LHs, and at the same time, pave the way for the use of hybrid *simonkolleite*-like structures as catalytic nanoreactors, of interest in the synthesis of carbon-based nanocomposites for energy storage and conversion.[17]

Acknowledgements

This work was supported by the European Research Council (ERC Starting Grant No. 2D-PnictoChem 804110 to G.A. and ERC Advanced Grant Mol-2D 788222 to E.C.), the Spanish MICINN (PID2019-111742GA-I00, project MAT2017-89993-R co-financed by FEDER and Unit of Excellence "Maria de Maeztu" CEX2019-000919-M), and the Generalitat Valenciana (CIDEGENT/2018/001 to G.A., Prometeo/2017/066, and iDiFEDER/2018/061 co-financed by FEDER). The authors thank Dr. G. Agustí and Dr. J. M. Martínez for magnetic measurements. V.O. is member of ALN.

Conflict of Interest

The authors declare no conflict of interest.

Keywords

2D materials, gas chromatography, hybrid materials, layered hydroxides, mass spectrometry, thermal stability, thermogravimetric analysis.

References

1. P. Gómez-Romero, C. Sanchez, in Functional Hybrid Materials, Wiley-VCH, Weinheim 2005, chap. 1, pp. 1– 14.
2. L. Nicole, L. Rozes, C. Sanchez, Adv. Mater. 2010, 22, 3208.
3. L. Nicole, C. Laberty-Robert, L. Rozes, C. Sanchez, Nanoscale 2014, 6, 6267.
4. C. Taviot-Guého, V. Prévot, C. Forano, G. Renaudin, C. Mousty, F. Leroux, Adv. Funct. Mater. 2018, 28, 1703868.
5. G. Rogez, C. Massobrio, P. Rabu, M. Drillon, Chem. Soc. Rev. 2011, 40, 1031.
6. P. Rabu, E. Delahaye, G. Rogez, Nanotechnol. Rev. 2015, 4, 557.

7. J. Azadmanjiri, J. Wang, C. C. Berndt, A. Yu, J. Mater. Chem. A 2018, 6, 3824.
8. R. Patel, J. Tae Park, M. Patel, J. Kumar Dash, E. Bhoje Gowd, R. Karpoormath, A. Mishra, J. Kwak, J. Hak Kim, J. Mater. Chem. A 2018, 6, 12.
9. I. Roger, M. A. Shipman, M. D. Symes, Nat. Rev. Chem. 2017, 1, 0003.
10. C. Tan, X. Cao, X.-J. Wu, Q. He, J. Yang, X. Zhang, J. Chen, W. Zhao, S. Han, G.-H. Nam, M. Sindoro, H. Zhang, *Chem. Rev.* 2017, 117, 6225.
11. Y. Liu, N. O. Weiss, X. Duan, H.-C. Cheng, Y. Huang, X. Duan, *Nat. Rev. Mater.* 2016, 1, 16042.
12. W. Zhang, Q. Wang, Y. Chen, Z. Wang, A. T. S. Wee, *2D Mater.* 2016, 3, 022001.
13. Q. Wang, D. O'Hare, *Chem. Rev.* 2012, 112, 4124.
14. F. Li, X. Duan, in *Layered Double Hydroxides* (Eds.: X. Duan, D. G. Evans), Springer, Berlin/Heidelberg, 2006, pp. 193– 223.
15. G. Abellán, J. L. Jordá, P. Atienzar, M. Varela, M. Jaafar, J. Gómez-Herrero, F. Zamora, A. Ribera, H. García, E. Coronado, *Chem. Sci.* 2015, 6, 1949.
16. X. Li, D. Du, Y. Zhang, W. Xing, Q. Xue, Z. Yan, *J. Mater. Chem. A* 2017, 5, 15460.
17. J. Romero, H. Prima-Garcia, M. Varela, S. G. Miralles, V. Oestreicher, G. Abellán, E. Coronado, *Adv. Mater.* 2019, 31, 1900189.
18. J. A. Carrasco, A. Seijas-Da Silva, V. Oestreicher, J. Romero, B. G. Márkus, F. Simon, B. J. C. Vieira, J. C. Waerenborgh, G. Abellán, E. Coronado, *Chem. Eur. J.* 2020, 26, 6504.
19. R. Ma, Z. Liu, K. Takada, K. Fukuda, Y. Ebina, Y. Bando, T. Sasaki, *Inorg. Chem.* 2006, 45, 3964.
20. D. Hunt, M. Jobbagy, D. A. Scherlis, *Inorg. Chem.* 2018, 57, 4989.
21. V. Oestreicher, D. Hunt, R. Torres-Cavanillas, G. Abellán, D. A. Scherlis, M. Jobbágy, *Inorg. Chem.* 2019, 58, 9414.
22. J. R. Neilson, D. E. Morse, B. C. Melot, D. P. Shoemaker, J. A. Kurzman, R. Seshadri, *Phys. Rev. B* 2011, 83, 094418.
23. V. Oestreicher, D. Hunt, C. Dolle, P. Borovik, M. Jobbágy, G. Abellán, E. Coronado, Chem. Eur. J. 2020, https://doi.org/10.1002/chem.202003593.
24. G. Abellán, C. Martí-Gastaldo, A. Ribera, E. Coronado, Acc. Chem. Res. 2015, 48, 1601.
25. J. Romero, M. Varela, M. Assebban, V. Oestreicher, A. Guedeja-Marrón, J. L. Jorda, G. Abellán, E. Coronado, *Chem. Sci.* 2020, 11, 7626.
26. V. Oestreicher, M. Jobbágy, *Langmuir* 2013, 29, 12104.
27. N. Arencibia, V. Oestreicher, F. A. Viva, M. Jobbágy, *RSC Adv.* 2017, 7, 5595.
28. V. Oestreicher, I. Fábregas, M. Jobbágy, *J. Phys. Chem. C* 2014, 118, 30274.
29. V. Oestreicher, M. Jobbágy, *Chem. Eur. J.* 2019, 25, 12611.
30. V. Oestreicher, M. Jobbágy, *Chem. Commun.* 2017, 53, 3466.
31. J. A. Dean, N. A. Lange, *Lange's Handbook of Chemistry*, McGraw-Hill, New York 1999.
32. M. Shabanian, M. Hajibeygi, A. Raeisi, in *Layered Double Hydroxide Polymer Nanocomposites* (Eds.: S. Thomas, S. Daniel), Woodhead Publishing, Oxford 2020, pp. 77– 101.
33. R. C. Mehrotra, R. Bohr, in *Metal Carboxylates*, Academic Press, New York 2006.
34. Y. Lu, J. D. Miller, *J. Coll. Interface Sci.* 2002, 256, 41.
35. Z. Liu, R. Ma, M. Osada, K. Takada, T. Sasaki, *J. Am. Chem. Soc.* 2005, 127, 13869.

36. V. Oestreicher, D. Hunt, M. Mizrahi, F. G. Requejo, M. Jobbágy, *Chem. Eur. J.* 2020, https://doi.org/10.1002/chem.202001944.
37. J. A. Carrasco, S. Cardona-Serra, J. M. Clemente-Juan, A. Gaita-Ariño, G. Abellán, E. Coronado, *Inorg. Chem.* 2018, 57, 2013.
38. A. S.-D. Silva, R. Sanchis-Gual, J. A. Carrasco, V. Oestreicher, G. Abellán, E. Coronado, *Batteries Supercaps* 2020, 3, 499.
39. G. Abellán, J. A. Carrasco, E. Coronado, *Inorg. Chem.* 2013, 52, 7828.
40. E. Conterosito, L. Palin, D. Antonioli, D. Viterbo, E. Mugnaioli, U. Kolb, L. Perioli, M. Milanesio, V. Gianotti, *Chem. Eur. J.* 2015, 21, 14975.
41. J. A. Carrasco, J. Romero, M. Varela, F. Hauke, G. Abellán, A. Hirsch, E. Coronado, *Inorg. Chem. Front.* 2016, 3, 478.
42. G. Abellán, M. Schirowski, K. F. Edelthalhammer, M. Fickert, K. Werbach, H. Peterlik, F. Hauke, A. Hirsch, *J. Am. Chem. Soc.* 2017, 139, 5175.
43. J. A. Carrasco, R. Sanchis-Gual, A. S.-D. Silva, G. Abellán, E. Coronado, Chem. Mater. 2019, 31, 6798.
44. G. Abellán, E. Coronado, C. Martí-Gastaldo, A. Ribera, J. F. Sánchez-Royo, Chem. Sci. 2012, 3, 1481.
45. Z. Li, M. Shao, L. Zhou, R. Zhang, C. Zhang, M. Wei, D. G. Evans, X. Duan, *Adv. Mater.* 2016, 28, 2337.